



1 **Temporary stratification promotes large greenhouse gas emissions in a shallow eutrophic lake**

2 Thomas A Davidson^{1,2}, Martin Søndergaard^{1,2,3}, Joachim Audet^{1,2}, Eti Levi¹, Chiara Esposito^{1,2}, Anders
3 Nielsen⁴.

4

5 ¹ Lake Ecology, Department of Ecoscience, Aarhus University, Denmark

6 ² WATEC Aarhus University Centre for Water Technology, Aarhus University, Denmark

7 ³ Sino-Danish Centre for Education and Research (SDC), Beijing, China

8 ⁴ WaterITech Aps, Døjsøvej 1, 8660 Skanderborg, Denmark

9 Corresponding author: Thomas A Davidson, C. F. Møllers Alle 4-6, DK-8000 Aarhus C, Denmark, e-
10 mail: thd@ecos.au.dk

11

12

13

14

15 **Abstract**

16 Shallow lakes and ponds undergo frequent temporary thermal stratification. How this affects greenhouse
17 gas (GHG) emissions is moot, with both increased and reduced GHG emissions hypothesised. Here,
18 weekly estimation of GHG emissions were combined with high-resolution temperature and oxygen
19 profiles of an 11 hectare shallow lake to investigate how thermal stratification shapes GHG emissions.
20 There were three main stratification periods with profound anoxia in the bottom waters occurring quickly
21 upon isolation from the atmosphere. Average diffusive emission of methane (CH₄) and nitrous oxide
22 (N₂O) were larger and more variable in stratified phase, whereas carbon dioxide (CO₂) was on average
23 lower. CH₄ ebullition was an order of magnitude greater in the stratified phase. In addition, there was a
24 large efflux of CH₄ and CO₂ when the lake mixed after periods of extended (circa 14 days) thermal
25 stratification. These two turnover events were estimated to have released the majority of the CH₄ emitted



26 between May and September. These results highlight the role of turnover emissions resulting from
27 temporary thermal stratification and also the need high frequency measurements of GHG emission in
28 order to accurately characterise emissions from these temporarily stratifying lakes.

29

30

31 Keywords: Climate change; lake stratification; methane; carbon dioxide; nitrous oxide; climate
32 feedbacks

33



34 **1. Introduction**

35 Fresh waters are key sites for the processing of greenhouse gases (GHG), methane (CH₄), carbon dioxide
36 (CO₂) and nitrous oxide (N₂O). Shallow lakes in particular, have been identified as hot spots of CH₄
37 release, particularly when ebullition is taken into account (Davidson et al., 2018; Aben et al., 2017). The
38 certainty that fresh waters are large emitters of GHGs contrasts sharply with the uncertainties associated
39 with the quantities emitted and this is in large part due to historical paucity of measurements (Cole, 2013).
40 A recent study identified the highly variable emissions from lakes and ponds which make a large
41 proportion of total emissions (Rosentreter et al., 2021). A dearth of measurement combined with these
42 highly variable emissions makes determining the drivers and controls of those emissions a challenge,
43 which in turn makes predicting future emissions difficult.

44

45 The current and future effects of climate change on lakes in general and on their GHG emissions are
46 relevant questions as there is potential for positive feedbacks and synergies with other human impacts
47 such as eutrophication (Davidson et al., 2018; Beaulieu et al., 2019; Delsontro et al., 2016; Meerhoff et
48 al., 2022). Taking a broad metabolic theory of ecology approach temperature increases should promote
49 methanogenesis and shift the balance from primary production to respiration increasing CO₂ emission at
50 cellular and ecosystem scale (Yvon-Durocher et al., 2010). However, empirical and experimental data
51 indicate that temperature is not the sole control of primary production and methanogenesis. In particular
52 eutrophication, and the promotion of large algal crop, has been associated with increased emissions of
53 CH₄ and N₂O (Delsontro et al., 2016) both by diffusion and ebullition (Zhou et al., 2019). Furthermore, in
54 what is globally the most abundant lake type, small shallow lakes, where macrophytes can colonise large
55 areas of the lake bed, the identity of the dominant primary producer may be more important than
56 temperature in shaping GHG dynamics (Davidson et al., 2015; Davidson et al., 2018; Bastviken et al.,
57 2023).

58



59 Climate change effects on lakes are not limited to increases in average temperatures and lengthening of
60 the growing season. Increases in both the frequency and intensity of heat waves are predicted, which will
61 promote the warming of surface waters and in turn make permanent and temporary thermal stratification
62 of lakes more likely (Woolway and Merchant, 2019), even in lakes typically classified as non-stratifying
63 (Kirillin and Shatwell, 2016). Emissions of gases, in particular CH₄, that accumulate in the isolated
64 bottom waters of a stratified lake, occurs upon mixing and can make very significant contributions to
65 cumulative emissions (Schubert et al., 2012). High-resolution studies of sites that undergo temporary
66 stratification are, however, rare (Søndergaard et al., 2023). In terms of its effects on GHG dynamics, there
67 are potentially antagonistic processes at work in a stratified lake. On the one hand the ‘shield effect’
68 results in lower temperatures at the sediment surface slowing down metabolic processes that scale with
69 temperature, i.e. methanogenesis and mineralization of organic carbon, reducing emission and promoting
70 carbon burial. On the other hand, anoxia at the sediment surface may shift processes towards
71 fermentation, increasing the proportion and total amount of CH₄ produced and perhaps reducing C burial
72 (Bartosiewicz et al., 2019). Recent work combining empirical observations and models has suggested that
73 shielding effects are larger than the anoxia effects and that stratification, in general, increases C burial and
74 reduces GHG emissions. The stratification induced isolation of bottom waters was reported to lead to
75 reduced ebullition of CH₄ and a shift to diffusive pathways (Bartosiewicz et al., 2015). It might, however,
76 be predicted that in shallow lakes stratification would lead to much larger CH₄ release as anoxic
77 conditions would limit CH₄ oxidation by CH₄ oxidizing bacteria (MOBs) (Bastviken et al., 2008). There
78 may also be other factors with the potential to increase GHG emission, such as sediment organic content
79 and lake trophic status (Delsontro et al., 2016), which may interact with stratification patterns in shaping
80 GHG emissions.

81

82 In this study, we used data from a shallow lake with high frequency measurements of temperature profiles
83 combined with weekly measurements of dissolved gas concentrations in the surface and bottom waters
84 and continuous measurement of ebullitive emissions of CH₄ to track the effects of lake stratification on



85 GHG emissions. The key question was how ebullitive and diffusive fluxes of the key GHGs: CH₄, CO₂
86 and N₂O respond to temporary thermal stratification.

87

88 **2. Materials and methods.**

89 **2.1 Study site**

90 Ormstrup lake (lat 56.326°, lon 9.639°) (Fig.1) (depth map with GHG sampling locations) is an 11 ha,
91 shallow lake (average depth 3.4 m), with a maximum depth of 5.5 m, with a relatively long hydraulic
92 retention time (> 1 year). The lake is eutrophic with high TP and chlorophyll-a (Table 1; Søndergaard et
93 al., 2022) with very sparse occurrence of submerged plants.

94

95 **2.2 Depth profiling and high frequency measurements**

96 In June 2020 a Nexsens (NexSens Technology, Fairborn, OH, USA) CB-450 data buoy system
97 (https://www.nexsens.com/pdf/CB450_datasheet.pdf) was deployed at the deepest point of the lake
98 equipped with a Nexsens TS210 thermistor string https://www.nexsens.com/pdf/TS210_datasheet.pdf
99 with temperature nodes measuring temperature at 4 levels; one sensor “in air”, ca. 5 cm above the water
100 surface, at the buoy and three sensors at -1, -2, -3 meters, respectively relative to the water surface. In
101 addition two Aqua TROLL 500 (In-Situ, Fort Collins, CO, USA) multi-sondes were mounted near the
102 surface (-1.0 meters) and at deeper water depth (-3.8 meters). The near surface and deeper water sonde
103 were configured with sensors to measure dissolved oxygen (DO) and temperature (Tw). The optical
104 sensors were calibrated according to manufacture guidelines and checked on a weekly basis.

105

106 The optical sensors of the Aqua TROLL 500 have a built-in wiper mechanism to clean sensor heads to
107 hamper bio-fouling. The wiper function was enabled to perform cleaning in sync with sensor
108 measurements, hence every 15 minutes. In addition, manual cleaning of sensor heads was done every



109 week, while routine manual field monitoring was carried out at the lake. Prior to the deployment of the
110 buoy, and as a validation exercise for the buoy data, weekly manual profiles of DO and Tw were collected
111 at the deepest point.

112

113 Periods of stratification were defined by a greater than 2 °C difference between the surface and bottom
114 waters and DO below 0.5 mg l⁻¹ at the time of the weekly manual profiling of the system. The high
115 frequency measurements were used to confirm the patterns. During periods of stratification, there may be
116 partial mixing events where some of the water column mixes, but the bottom waters remain undisturbed.

117

118 **2.3 Water chemistry**

119 Water samples for the analysis of Chlorophyll-a were collected weekly from the 20. April 2020 from
120 surface (-0.5 m) water at station 3 (Fig. 1) and analysed according to Danish standard procedures
121 (Søndergaard et al., 2005). Depth profiles of temperature, electrical conductivity (EC) and dissolved
122 oxygen (DO) were measured manually with an Aqua TROLL 500 probe from every -0.5 or -1 m down to
123 -5 m depth).

124

125 **2.4 Greenhouse gas sampling**

126 **2.4.1 Dissolved concentration**

127 Samples of dissolved concentrations of CH₄, CO₂ and N₂O were collected weekly from the 20. April 2020
128 from surface waters and weekly from surface and bottom water from the 26. May 2020. The samples
129 were taken using head-space equilibration after (Mcauliffe, 1971), where 20 ml of water was collected
130 from just below the water surface and 20 ml of N₂ was introduced as a headspace in a 60-ml syringe and
131 then shaken vigorously for one minute. The 20 ml headspace was then transferred to a 12-ml pre
132 evacuated glass vial.



133

134 Samples were collected between 12. May 2020–15. October 2020 which is 126 days and cover the majority
135 of the growing season.

136 Gas concentrations in the headspace were determined on a dual-inlet Agilent 7890 GC system interfaced
137 with a CTC CombiPal autosampler (Agilent, Nærum, Denmark) (Petersen et al., 2012). For the GC,
138 certified CO₂, CH₄ and N₂O standards were used for calibration and validation. Aqueous concentrations in
139 N₂O, CH₄ and CO₂ were calculated from the headspace gas concentrations according to Henry's law and
140 using Henry's constant corrected for temperature and salinity (Weiss, 1974; Weiss and Price, 1980;
141 Wiesenburg and Guinasso, 1979).

142 The fluxes of N₂O, CH₄ and CO₂ between the water and the overlying atmosphere were estimated as

$$143 \quad f_g = k_g(C_{wat,g} - C_{eq,g})$$

144 Where f_g is the flux of a specific gas g , k_g is the piston velocity of the gas and $C_{wat,g} - C_{eq,g}$ is the
145 gradient of concentration between the concentration of gas dissolved in the water ($C_{wat,g}$) and the
146 concentration of gas the water would have at equilibrium with the atmosphere ($C_{eq,g}$).

147 We calculated a gas transfer velocity k_{600} for each sampling occasion using the relationship based on
148 windspeed described in (Cole and Caraco, 1998).

$$149 \quad k_{600} = 2.07 + 0.215U_{10}^{1.7}$$

150 U_{10} is the mean daily windspeed at 10m (m s⁻¹) obtained from the Danish meteorological institute
151 (DMI; 20x20 km grid data)

152

153

$$154 \quad k_g = k_{600} \left(\frac{Sc_g}{600} \right)^x$$

155



156 Sc_g is the Schmidt number (Wanninkhof, 1992) of the specific gas g . We chose $x = -2/3$ as this factor is
157 used for smooth liquid surface (Deacon, 1981).

158

159 Daily flux rates were calculated using linear interpolation of the weekly surface measurements from each
160 of the sampling points. Total diffusive surface water fluxes were calculated by taking an average of the
161 daily flux rate from the 12. May 2020 to the 13. October 2020. Then an average was taken for each location
162 and then an average of the 3 locations was multiplied by the area of the lake and the number of days covered
163 by the study, here 126 days was chosen to match the period over which ebullition was measured.

164

165 The total content of the gases in the lake's bottom waters were calculated from the concentration of the
166 gases per litre multiplied by an estimate of the volume of the water in the hypolimnion. The volume of
167 water in the hypolimnion was estimated from the lake profiles manually conducted on the day of
168 sampling. The top of the hypolimnion was determined by the depth below which oxygen was less than 0.5
169 mg l^{-1} . A detailed bathymetry of the lake allows the calculation of the area and therefore volume of water
170 that lies below a given depth. For the purposes of this study, it was assumed that all the gas in the
171 hypolimnion was released on turnover. This release was calculated from 30. June 2020 and from the 25.
172 August 2020, as they are the periods where complete mixing occurred and all the gases accumulated in
173 the bottom waters was likely to be released.

174

175

176 2.4.2 Ebullition

177 The ebullitive flux of CH_4 was estimated using a total of 40 floating chambers placed on 4 transects of 10
178 chambers each (Fig. 1). As the existing literature indicated that ebullition is lower as water depth
179 increases (Wik et al., 2013) the transects were placed to maximise the measurement of the low end of the
180 depth gradient on the shallower slopes of the western end of the lake (Fig. 1). The average and maximum



181 depth of each transect was T1: 293 cm and 472 cm; T2: 181 cm and 267, T3: 223 cm and 300 cm and T4
182 166 cm and 220 cm. The chambers were set on the 14. May 2020 and sampled every two weeks from that
183 date, and on one occasion after one week. Twenty ml of sample was taken from the floating chamber and
184 injected into a pre-evacuated 12 ml vial (exetainer, Labco). Gas concentrations were determined on the
185 same GC than described above (Petersen et al., 2012)

186 Ebullitive flux of CH₄ was estimated as:

$$187 \quad \frac{p_{gas} \times Vol_{bub}}{t \times A}$$

188 Where p_{gas} is the concentration of CH₄ in the gas that was trapped, Vol_{bub} is the volume of the chamber
189 (i.e. 7L), t is the time during which the samples was collected and A is the area of chamber (i.e. 0.075 m²).
190 A fraction of the CH₄ released via ebullition in the chamber will have re-dissolved in the water or might
191 leak through the chamber walls, thus underestimating the ebullitive flux. A study (Delsontro et al., 2016)
192 attempted to correct for this underestimation assuming that the CH₄ gas present in the bottle of the trap is
193 in equilibrium with the CH₄ dissolved in the water present in the bottle. This correction increased their
194 estimate of ebullitive flux by 2-5%. The chambers used here are even more vulnerable to the diffusion of
195 the bubble emissions from the chambers back into the water, due to their relatively large surface area of
196 water for the exchange of gas. In addition, there will be diffusion of CH₄ out of the chambers, estimated at
197 up to 100 ppm per day (Davidson & Audet, unpublished data). As the point at which the bubbles enter the
198 chamber is unknown it is difficult to estimate the degree of underestimation. The method is therefore a
199 suboptimal way of accurately estimating ebullition, as it is almost certainly an underestimate of the true
200 flux. However, the method is easy to apply and so can be used for longer periods, as it was here, and extend
201 the temporal resolution of the data providing information of variation in ebullition in space and time. The
202 estimates of absolute emissions of ebullition must be treated with caution, we can be confident that they are
203 underestimates, just not the degree to which they are underestimates.

204



205 Total ebullitive flux from the lake was calculated by taking a mean of the emissions from each transect over
206 the 126 day period. Then taking an average of the means of four transects and multiplying this by the time
207 of deployment of the chambers in days, which was 126 days, and by the area of the lake. This gives a total
208 ebullitive flux of CH₄ for the lake over the period of measurement.

209

210 The three different flux types, surface diffusion, ebullition and turnover emission were then converted in
211 comparable units of total lakes emissions (as g or kg of gas) over the studied period and also converted into
212 CO₂-equivalents using a conversion factor related to their 100 year global warming potential (GWP) of 28
213 for CH₄ and 298 for N₂O.

214

215 **3. Results**

216 **3.1 Lake physical and chemical characteristics**

217 Depth profiles measured weekly from April show that stratification was initiated by the 26. May 2020 this
218 may have broken down briefly and established again, visible in the temperature sensors for the buoy on
219 the 5. June 2020 (Fig. 2). There were then 12 days of mixing followed by stable period of stratification
220 with onset the 14. June 2020 and a duration of 16 days until a mixing event around the 30. June 2020. The
221 following two weeks had cooler water and a mixed water column, hereafter a ca. 6 day period of
222 stratification from the 15. to 21. July 2020. A mixed phase of two weeks then followed until stratification
223 reestablished on 4. August 2020 and persisted until the end of August, partial mixing is indicated by the
224 buoy data from the 21. August 2020, but the weekly manual profile to deeper water indicate that full
225 mixing did not occur until after the 25. August 2020. The effects of the stratification and mixing events on
226 the high frequency DO data measured at -3.8 m are clear, with rapid deoxygenation occurring after the
227 onset of stratification and oxic bottom waters returning when the lake mixed (Fig. 2). The pattern in
228 chlorophyll-a also follow, to some degree, those of stratification, with the exception of early spring.



229 Chlorophyll-a values were extremely high in spring peaking at the start of June 2020 and falling gradually
230 (Fig. 2). During the periods of stratification chlorophyll biomass was lower, likely limited by nitrogen
231 (Søndergaard et al., 2023) and when a mixing even occurred the values increased, which is particularly
232 evident in the July mixing periods (Fig. 2).

233

234 **3.2 Concentrations of dissolved gases and fluxes from the surface waters.**

235 The concentrations of the dissolved gases showed great variation from near or below atmospheric
236 concentrations in some cases and up to an extremely high concentration (over 5 mg CH₄ C l⁻¹) in the
237 bottom waters on the 30. June 2020. There was some spatial heterogeneity in the surface waters, with the
238 more littoral locations showing the greatest variation and the highest values (Figs. 3,4,5). In particular the
239 most littoral zone, where the water was shallower around 1 m in depth, showed the highest values just
240 prior to, or coincident with, the stratification turnover. Table 2 shows the mean diffusive flux of each gas
241 over the sampling period along with the mean flux in mixed and stratified phases. For CO₂ there was a lot
242 of temporal variation in flux dynamics, though not a large difference between mixed and stratified phases
243 in terms of mean values (Table 2). There were some periods of CO₂ influx in spring and later summer and
244 these tended to coincide with the end of a mixed phase and the start of the stratification phase. N₂O
245 concentrations were generally low (Figs 4 & 5) with the lake being a source of N₂O in the spring period
246 and a sink or a very small source thereafter. The CH₄ concentration in the surface waters (Fig. 3) and the
247 calculated diffusive emissions are relatively low, but did increase in the stratification periods with higher
248 average values (Table 2 & Fig. 6). There was also some spatial variation with higher CO₂ and CH₄
249 diffusive emissions in the shallower sampling locations, both in stratified and mixed conditions (Fig. 6).

250

251 The most marked patterns in GHG concentration were evident in the bottom waters sampled at -4.5 m,
252 which accumulated to very large concentrations of CO₂ but particularly CH₄ in the periods of
253 stratification (Fig. 3 & 4). The ratio of CO₂ to CH₄ is illustrative in highlighting how stratification has



254 altered the biogeochemical processes in the hypolimnion with CH₄ production becoming more prevalent. .
255 For example on 30. June 2020 after 16 days of stratification the the ratio CO₂:CH₄ in the bottom waters
256 was 0.8, whereas 7 days later after the mixing event it was 187 at the same depth.

257

258 **3.3 Ebullitive fluxes**

259 The CH₄ bubble flux is presented here as mean values for each of the 4 transects ranged from 0.303 to
260 81.1 mg CH₄ C m² d⁻¹ for the individual transect over the growing season measurement. There is a very
261 clear impact of stratification on the ebullitive efflux of CH₄ with stratified periods showing markedly
262 higher levels of emission (Fig. 7 and Table 2). In addition there was a difference in average emissions
263 among the different transects, with those with lower average water depth (T2 & T4) having lower
264 emission than the transects with chambers over deeper water (T1 & T3) (Fig. 7). The samples collected
265 from the chambers reflect two weeks of bubble and diffusion collection and the quantification of the flux
266 is therefore an average of the period of chamber deployment, which was two weeks, or in one case a
267 single week (Fig. 7). This two week period on occasion covered both stratified and mixed phases and on
268 these occasions efflux was intermediate between purely mixed and stratified periods (Table 2 and Fig.
269 7).

270

271 **3.4 Total lake fluxes**

272 Scaling up the results to total flux of gases from the whole lake over the period of study and including the
273 estimated emissions from two turnover events show a very different effect of stratification on the balance
274 of types of emissions for the three gases. The majority of CH₄ emission (56%) result from the two short-
275 lived turnover events (Fig. 8), whereas their contribution to CO₂ and N₂O emission was 5% and 1%
276 respectively. Fluxes of CO₂ and N₂O were mostly diffusive, which represented 95% of emissions of both
277 gases. CH₄ diffusive flux was 14% of total emission whereas CH₄ ebullition was more than twice and
278 much representing 29% of total CH₄ emission. In terms of global warming potential CO₂ and CH₄



279 emission were comparable, but the contribution of the turnover efflux was the dominant factor for CH₄
280 emissions.

281

282 **4. Discussion**

283 The emission of CH₄ reported here (Table 2) showed great variation between the mixed and stratified
284 phases. The mean of the total emissions from Ormstrup in the stratified phase (58 mg CH₄-C m⁻² day⁻¹)
285 correspond relatively closely to the mean of the total emissions (ebullition plus diffusion) reported for
286 lakes in this size range (47 mg CH₄-C m⁻² day⁻¹), though they are well above the median value 15 mg
287 CH₄-C m⁻² day⁻¹ (Rosentreter et al., 2021). The data provide a clear answer to the question of how thermal
288 stratification affects GHG dynamics in shallow eutrophic lakes with an increase in total emissions
289 (diffusion, ebullition and turnover) during the stratified period (Table 2, Fig 9). Previous work, combining
290 observations and modelling suggested the opposite patterns (Bartosiewicz et al., 2019) as their study
291 suggested that the shielding effect results in cooler bottom waters and this reduce CH₄ production due to
292 the temperature dependence of CH₄ production (Bartosiewicz et al., 2016). This strong shielding effect
293 may apply in deeper lakes experiencing more stable stratification, or less eutrophic lakes, the result here
294 show, however, that stratification causes massive increases in GHG emissions.

295 Diffusive emissions did not on average show a strong stratification effect (Table 2). There were peaks in
296 emission of CH₄ and CO₂ at the end of stratification periods, particularly in the shallower water sampling
297 points (Fig. 6). Littoral zones can have markedly different GHG dynamics to deeper zones due to
298 shallower water having lower pressure (Wik et al., 2013), less time for CH₄ oxidation (Bastviken et al.,
299 2008) or abundant plants which influence a range of biogeochemical processes (Davidson et al., 2018;
300 Esposito et al., 2023). It is therefore possible that littoral zone dynamics could cause these differences.
301 However, the increase occurred at all three sampling points at the end of June 2020, which indicates a
302 more lake-wide driver and the peak may represent the start of mixing after stratification. Strong winds
303 were measured on the 29th and 30th June 2020 (Søndergaard et al., 2023) coincident with these increased



304 littoral emissions. These winds would have caused lateral movement of the surface water causing an
305 upwelling of bottom water, rich in CH₄ and CO₂, in the littoral margins at the opposite end of the lake.
306 Thus, whilst we do not have direct evidence it seems more likely that these increased emissions in the
307 littoral zone were not driven at least in part the partial mixing of the GHG rich bottom waters. In contrast
308 to the diffusive flux, the ebullitive emission of CH₄ shows a very clear response to stratification with an
309 order of magnitude difference in emissions between periods where the sampling reflected purely mixed
310 or stratified periods (Table 2 & Fig. 7). The two-week resolution of the sampling meant that some
311 samples covered both stratified and mixed phases and these samples had intermediate fluxes, as they
312 cover both low (mixed) and high emission (stratified) periods. The spatial variation in ebullition is also
313 illustrative of the impacts of stratification and the role of anoxia in shaping CH₄ fluxes. The two transects
314 with the largest mean and maximum depths (T1 and T3) had the largest emissions, with the deeper of the
315 two (T1) having the highest emissions and they saw the greatest relative increase during the stratification
316 phases. This pattern is the obverse of that found in other studies where bubble emissions were larger in
317 shallower water as higher pressure in deeper location means production rates of CH₄ need to be higher for
318 bubbles to form (Wik et al., 2013). Deeper water at Ormstrup experiences anoxia earlier and this appears
319 to cause locations with deeper water to have higher ebullition rates than shallower areas. This is at odds
320 with ideas stemming from the metabolic theory of ecology stating that temperature (Yvon-Durocher et al.,
321 2014) in particular at the sediment surface (Bartosiewicz et al., 2019) can be used to predict CH₄ efflux.
322 Whilst it is a fact that CH₄ production is temperature dependent at the cellular level, CH₄ emissions were
323 rather independent of the sediment temperature, for example in the first two weeks of July 2020 emissions
324 were low and the sediment surface temperature was relatively high. Thus, temperature alone is a poor
325 predictor of ecosystem scale CH₄ emissions.

326

327 It should be noted that the methods used to estimate bubble flux here, where floating chambers are
328 sampled every two weeks is a “less than perfect method”, which in most cases will underestimate
329 ebullitive flux. Logistical and financial constraints make continual sampling difficult and here we



330 balanced these constrains against the greater time required to apply more accurate methods, such as
331 bubble traps (Wik et al., 2013) or automatic flushing chambers (Bastviken et al., 2015). Such is the
332 variability of bubble flux in space and time that sampling campaigns covering days or weeks would
333 potentially give an even more inaccurate picture of emissions than the method used here. Thus, the
334 continuous monitoring of ebullition using chambers with known biases was deemed the least worst
335 method available, but we acknowledge the caveat that ebullitive emissions may be underestimated.
336

337 In addition to diffusive and ebullitive emissions the turnover flux, which consists of the gases
338 accumulated in the hypolimnion being released on turnover, was also estimated. There were two major
339 turnover events at the end of June and in late in August 2020, which were preceded by 16 and 22 days of
340 stratification, respectively. It was not possible to directly measure turnover flux, as they are relatively
341 discrete events where the efflux likely occurs over the course of just a few hours. Evidence of this is that
342 the complete oxygenation of the water column during the mixing event at the start of July 2020 took just a
343 few hours (Søndergaard et al., 2023). Thus, the efflux is estimated from the bottom concentration with the
344 assumption that all the CO₂ and CH₄ in the bottom water was released at turnover, which is potentially an
345 over estimate. Notwithstanding this uncertainty we can be confident the turnover flux represents a very
346 large proportion of the total emission of CH₄ emissions from Ormstrup Lake over the growing season. We
347 estimate it contributed more than 50 % of growing season CH₄ emissions and 5 % of CO₂ emissions. This
348 highlights a very significant, and generally unmeasured, contribution to GHG emissions from lakes
349 undergoing temporary stratification, which are among the most common lake type in Denmark.

350 Furthermore, stratification is increasingly recognised as prevalent in ponds and shallow lakes (Holgerson
351 et al., 2022) and it is likely to become more common with continued climate change impacts (Woolway
352 and Merchant, 2019). Predicting the response of GHG emissions in a warmer world is, however, not
353 straightforward, as stable stratification over the whole summer may have different impacts to the more
354 transient stratification patterns as observed here. Conversely, more frequent summer storms in climate
355 change predictions could also result in mixing events that could cause large turnover emissions.



356

357 The results here suggest that GHG dynamics were driven both directly and indirectly by the stratification
358 patterns and the anoxia it induced in the bottom waters. At Ormstrup Lake the thermal stratification of the
359 water column quickly led to anoxia, with only a matter of hours to days for the oxygen to be consumed
360 once the bottom waters were isolated (Fig. 2). The ratios of CO₂:CH₄ evidence how this promotes CH₄
361 over CO₂ production in the stratification phase (see Fig 9). In addition to promoting CH₄ production such
362 conditions would preclude, or severely limit, CH₄ oxidation, which has the potential to consume a large
363 proportion of CH₄ produced in the anoxic sediments (Bastviken et al., 2008). The raw emission data do
364 not provide any direct information on the balance of production versus oxidation, but the CO₂:CH₄
365 suggest there was marked shift to conditions where methanogenesis was the dominant process and there
366 was reduced CO₂ production. Studies have shown that CH₄ oxidation can consume large proportions of
367 the CH₄ produced under hypoxia (Saarela et al., 2019) and it is possible that there is intense CH₄ oxidation
368 occurring at the thermocline during the periods of stratification at Ormstrup lake , but this was not directly
369 measured at the lake. In addition to the more direct effects of anoxia there may be some indirect effects of
370 the patterns of stratification and mixing that promote greater GHG emissions. Søndergaard et al. (2023)
371 recently reported how nutrient dynamics at Ormstrup Lake were altered by the lake stratification and full
372 details can be found there, of relevance here is the impact on chlorophyll-a which saw a large spring peak
373 after which the abundance tracked the stratification and mixing regime, with a lag time. There was a
374 general reduction, or at least no increase as the stratification period progressed, perhaps due to nutrient
375 limitation in the epilimnion. Upon mixing there was generally an increase in chlorophyll-a, though the
376 weekly sampling resolution makes this difficult to assess. Chlorophyll-a and the labile dissolved organic
377 carbon (DOC) that result from abundant chlorophyll-a have been shown to be associated with higher
378 diffusive and ebullitive CH₄ emissions (Davidson et al., 2015; Beaulieu et al., 2019; West et al., 2012;
379 Zhou et al., 2019). It is not possible to say here whether a stable summer long stratification would have
380 led to decreased chlorophyll-a as nutrients became limiting due to their isolation in the bottom waters and
381 reliable high frequency chlorophyll-a data are required to convincingly demonstrate this phenomenon.



382 Notwithstanding these uncertainties it may be the case that the temporary stratification, interspersed with
383 mixing events, observed here represents a ‘sweet spot’ providing both the resources, i.e. chlorophyll-a and
384 the labile DOC it produces, and optimal conditions (anoxia) for CH₄ production.

385

386 The combination of high frequency data on water temperature and dissolved oxygen combined with
387 weekly measurements of GHGs increase the reliability of the findings presented here. Up until relatively
388 recently it has been assumed shallow lakes, such as Ormstrup lake, stratification is not an important
389 feature. Sampling has therefore focused on surface waters, using dissolved concentrations of gases or
390 floating chambers to characterise flux, e.g. (Davidson et al., 2015; Audet et al., 2020; Peacock et al.,
391 2021). Thus, most studies have overlooked bottom waters and do not have the temporal resolution
392 required to capture turnover flux emissions from surface measurements. Furthermore, whilst many studies
393 now include estimates of bubble emissions of CH₄ e.g. (Bergen et al., 2019), the necessary temporal
394 resolution to accurately characterise ebullitive emission is not well established. The finding here indicated
395 that in such dynamic systems near continuous measurement is desirable and that short term collection
396 over one or two days could provide massive, over or under estimate of CH₄ ebullition.

397

398 Our results show very large temporal variation in emissions of all three gases, but in particular CO₂ and
399 CH₄, and this highlights the need for high frequency measurements to accurately characterize emissions
400 from lakes. Even the weekly frequency of the sampling in this study was not sufficient to directly measure
401 all the emission pathways and turnover flux had to be inferred from bottom water calculations. These data
402 show that to capture the extent of GHG emissions from lakes it is vital we include all forms of flux,
403 including ebullition and turnover flux. Recent work has highlighted the fact that most emissions (over
404 50%) from fresh waters come from highly variable systems (Rosentreter et al., 2021), with the mean and
405 median emission rates of CH₄ differing greatly indicating a few large emitters are responsible for a large
406 proportion of emissions. The sampling frequency applied here is rare, if a more standard resolution of
407 monthly measurements was applied the emissions estimate of all the gases, but in particular CH₄, would



408 be highly dependent on what phase of the stratification was captured. As an example, a monthly sampling
409 frequency could potentially miss all the stratification peaks - consequently massively underestimating
410 emissions, whereas a different sampling frequency could catch a number of peaks and giving a much
411 higher estimate. Thus, the same sampling frequency on the same lake, but timed differently could lead to
412 conclusions of highly variable emissions. Thus, it seems in these highly dynamic systems that if
413 temporarily stratification may occur in summer, high frequency measurements are required to accurately
414 estimate emissions. This is logistically challenging but the current advances in the use of automatic
415 flushing chambers (Bastviken et al., 2020) may provide the potential for affordable high spatial and
416 temporal resolution measurement of GHG dynamics. This is a requisite for understanding the drivers of
417 GHG dynamic, which is required for being able to predict how they will respond in a range of scenarios
418 related to land use, climate change and management interventions.

419

420 **Code/data availability**

421 The datasets generated during and/or analysed during the current study are not publicly available as they
422 form part of ongoing research projects but are available from the corresponding author on reasonable
423 request and will be made publicly available later in the research project.

424

425 **Author contributions**

426 MS secured the funding for the wider lake restoration research project supplying the data. TAD, MS and
427 JA conceptualized the gas study. TAD and AN established the buoy and sensor system. EL, CE, TAD, JA
428 collected and analysed the data. TAD wrote the paper and all authors commented on earlier versions and
429 read and approved the final draft.

430 **Competing interests**

431 The authors declare that they have no conflicts of interest.





433 Acknowledgement

434 We thank our crack technician team of Lene Vigh, Malene Kragh, Dorte Nedegaard and Dennis Hansen
435 for their extreme competence on the lab and the field. We acknowledge Theis Kragh for the depth map of
436 the lake already published in Søndergaard et al. 2022. We are very grateful to the Poul Due Jensen
437 Fonden for providing great support for this work and the Ormstrup project generally. TAD and CE were
438 also supported by GREENLAKES (No. 9040-00195B) and The European Union's Horizon 2020 research
439 and innovation programmes under grant agreement No 869296—The PONDERFUL Project.

440

441

442 References

- 443 Aben, R. C. H., Barros, N., van Donk, E., Frenken, T., Hilt, S., Kazanjian, G., Lamers, L. P. M., Peeters, E. T.
444 H. M., Roelofs, J. G. M., de Senerpont Domis, L. N., Stephan, S., Velthuis, M., Van de Waal, D. B., Wik, M.,
445 Thornton, B. F., Wilkinson, J., DelSontro, T., and Kosten, S.: Cross continental increase in methane
446 ebullition under climate change, *Nat. Comms.*, 8, 1682, <https://doi.org/10.1038/s41467-017-01535-y>,
447 2017.
- 448 Audet, J., Carstensen, M. V., Hoffmann, C. C., Lavaux, L., Thiemer, K., and Davidson, T. A.: Greenhouse
449 gas emissions from urban ponds in Denmark, *Inland Waters*, 1-13,
450 <https://doi.org/10.1080/20442041.2020.1730680>, 2020.
- 451 Bartosiewicz, M., Laurion, I., and MacIntyre, S.: Greenhouse gas emission and storage in a small shallow
452 lake, *Hydrobiologia*, 757, 101-115, <https://doi.org/10.1007/s10750-015-2240-2>, 2015.
- 453 Bartosiewicz, M., Laurion, I., Clayer, F., and Maranger, R.: Heat-Wave Effects on Oxygen, Nutrients, and
454 Phytoplankton Can Alter Global Warming Potential of Gases Emitted from a Small Shallow Lake, *Environ.*
455 *Sci. Technol.*, 50, 6267-6275, <https://pubs.acs.org/doi/10.1021/acs.est.5b06312>, 2016.
- 456 Bartosiewicz, M., Przytulska, A., Lapierre, J.-F., Laurion, I., Lehmann, M. F., and Maranger, R.: Hot tops,
457 cold bottoms: Synergistic climate warming and shielding effects increase carbon burial in lakes, *Limnol.*
458 *Oceanogr. Lett.*, 4, 132-144, <https://doi.org/10.1002/lo12.10117>, 2019.
- 459 Bastviken, D., Cole, J. J., Pace, M. L., and Van de Bogert, M. C.: Fates of methane from different lake
460 habitats: Connecting whole-lake budgets and CH₄ emissions, *J. Geophys. Res.*, 113, G02024,
461 <https://doi.org/10.1029/2007JG000608>, 2008.
- 462 Bastviken, D., Nygren, J., Schenk, J., Parellada Massana, R., and Duc, N. T.: Technical note: Facilitating the
463 use of low-cost methane (CH₄) sensors in flux chambers – calibration, data processing, and an open-
464 source make-it-yourself logger, *Biogeosciences*, 17, 3659-3667, [https://doi.org/10.5194/bg-17-3659-](https://doi.org/10.5194/bg-17-3659-2020)
465 [2020](https://doi.org/10.5194/bg-17-3659-2020), 2020.



- 466 Bastviken, D., Sundgren, I., Natchimuthu, S., Reyier, H., and Gålfalk, M.: Technical Note: Cost-efficient
467 approaches to measure carbon dioxide fluxes and concentrations in terrestrial and aquatic
468 environments using mini loggers, *Biogeosciences*, 12, 3849-3859,
469 <https://doi.org/10.5194/bg-12-3849-2015>, 2015.
- 470 Bastviken, D., Treat, C. C., Pangala, S. R., Gauci, V., Enrich-Prast, A., Karlson, M., Gålfalk, M., Romano, M.
471 B., and Sawakuchi, H. O.: The importance of plants for methane emission at the ecosystem scale, *Aquat.*
472 *Bot.*, 184, 103596, <https://doi.org/10.1016/j.aquabot.2022.103596>, 2023.
- 473 Beaulieu, J. J., DelSontro, T., and Downing, J. A.: Eutrophication will increase methane emissions from
474 lakes and impoundments during the 21st century, *Nat. Comms.*, 10, 1-5,
475 <https://doi.org/10.1038/s41467-019-09100-5>, 2019.
- 476 Bergen, T. J. H. M., Barros, N., Mendonça, R., Aben, R. C. H., Althuisen, I. H. J., Huszar, V., Lamers, L. P.
477 M., Lüring, M., Roland, F., and Kosten, S.: Seasonal and diel variation in greenhouse gas emissions from
478 an urban pond and its major drivers, *Limnol. Oceanogr.*, 64, 2129-2139,
479 <https://doi.org/10.1002/lno.11173>, 2019.
- 480 Cole, J.: Freshwater in flux, *Nat. Geosci.*, 6, 13-14, <https://doi.org/10.1038/ngeo1696>, 2013.
- 481 Cole, J. J. and Caraco, N. F.: Atmospheric exchange of carbon dioxide in a low-wind oligotrophic lake
482 measured by the addition of SF₆, *Limnol. Oceanogr.*, 43, 647-656,
483 <https://doi.org/10.4319/lo.1998.43.4.0647>, 1998.
- 484 Davidson, T. A., Audet, J., Jeppesen, E., Landkildehus, F., Lauridsen, T. L., Søndergaard, M., and
485 Syvaranta, J.: Synergy between nutrients and warming enhances methane ebullition from experimental
486 lakes, *Nat. Clim. Chang.*, 8, 156-160, <https://doi.org/10.1038/s41558-017-0063-z>, 2018.
- 487 Davidson, T. A., Audet, J., Svenning, J.-C. C., Lauridsen, T. L., Søndergaard, M., Landkildehus, F., Larsen, S.
488 E., and Jeppesen, E.: Eutrophication effects on greenhouse gas fluxes from shallow-lake mesocosms
489 override those of climate warming, *Glob. Chang. Biol.*, 21, 4449-4463,
490 <https://doi.org/10.1111/gcb.13062>, 2015.
- 491 Deacon, E. L.: Sea-air gas transfer: The wind speed dependence, *Bound.- Layer. Meteorol.*, 21, 31-37,
492 <https://doi.org/10.1007/bf00119365>, 1981.
- 493 DelSontro, T., Boutet, L., St-Pierre, A., del Giorgio, P. A., and Prairie, Y. T.: Methane ebullition and
494 diffusion from northern ponds and lakes regulated by the interaction between temperature and system
495 productivity, *Limnol. Oceanogr.*, 61, S62-S77, <http://doi.wiley.com/10.1002/lno.10335>, 2016.
- 496 Esposito, C., Nijman, T. P. A., Veraart, A. J., Audet, J., Levi, E. E., Lauridsen, T. L., and Davidson, T. A.:
497 Activity and abundance of methane-oxidizing bacteria on plants in experimental lakes subjected to
498 different nutrient and warming treatments, *Aquat. Bot.*, 185, 103610,
499 <https://doi.org/10.1016/j.aquabot.2022.103610>, 2023.
- 500 Holgerson, M. A., Richardson, D. C., Roith, J., Bortolotti, L. E., Finlay, K., Hornbach, D. J., Gurung, K., Ness,
501 A., Andersen, M. R., Bansal, S., Finlay, J. C., Cianci-Gaskill, J. A., Hahn, S., Janke, B. D., McDonald, C.,
502 Mesman, J. P., North, R. L., Roberts, C. O., Sweetman, J. N., and Webb, J. R.: Classifying Mixing Regimes
503 in Ponds and Shallow Lakes, *Water Resour. Res.*, 58, e2022WR032522,
504 <https://doi.org/10.1029/2022WR032522>, 2022.
- 505 Kirillin, G. and Shatwell, T.: Generalized scaling of seasonal thermal stratification in lakes, *Earth Sci. Rev.*,
506 161, 179-190, <https://doi.org/10.1016/j.earscirev.2016.08.008>, 2016.



- 507 McAuliffe, C.: Gas chromatographic determination of solutes by multiple phase equilibrium, *Chem*
508 *Technol*, 1, 46-51, 1971.
- 509 Meerhoff, M., Audet, J., Davidson, T. A., De Meester, L., Hilt, S., Kosten, S., Liu, Z., Mazzeo, N., Paerl, H.,
510 Scheffer, M., and Jeppesen, E.: Feedbacks between climate change and eutrophication: revisiting the
511 allied attack concept and how to strike back, *Inland Waters*, 1-42,
512 <https://doi.org/10.1080/20442041.2022.2029317>, 2022.
- 513 Peacock, M., Audet, J., Bastviken, D., Cook, S., Evans, C. D., Grinham, A., Holgerson, M. A., Högbom, L.,
514 Pickard, A. E., Zieliński, P., and Futter, M. N.: Small artificial waterbodies are widespread and persistent
515 emitters of methane and carbon dioxide, *Glob. Chang. Biol.*, 27, 5109-5123,
516 <https://doi.org/10.1111/gcb.15762>, 2021.
- 517 Petersen, S. O., Hoffmann, C. C., Schäfer, C. M., Blicher-Mathiesen, G., Elsgaard, L., Kristensen, K.,
518 Larsen, S. E., Torp, S. B., and Greve, M. H.: Annual emissions of CH₄ and N₂O, and ecosystem respiration,
519 from eight organic soils in Western Denmark managed by agriculture, *Biogeosciences*, 9, 403-422,
520 <https://doi.org/10.5194/bg-9-403-2012>, 2012.
- 521 Rosentreter, J. A., Borges, A. V., Deemer, B. R., Holgerson, M. A., Liu, S., Song, C., Melack, J., Raymond, P.
522 A., Duarte, C. M., Allen, G. H., Olefeldt, D., Poulter, B., Battin, T. I., and Eyre, B. D.: Half of global methane
523 emissions come from highly variable aquatic ecosystem sources, *Nat. Geosci.*, 14, 225-230,
524 <https://doi.org/10.1038/s41561-021-00715-2>, 2021.
- 525 Saarela, T., Rissanen, A. J., Ojala, A., Pumpanen, J., Aalto, S. L., Tirola, M., Vesala, T., and Jäntti, H.: CH₄
526 oxidation in a boreal lake during the development of hypolimnetic hypoxia, *Aquat. Sci.*, 82, 19,
527 <https://doi.org/10.1007/s00027-019-0690-8>, 2019.
- 528 Schubert, C. J., Diem, T., and Eugster, W.: Methane Emissions from a Small Wind Shielded Lake
529 Determined by Eddy Covariance, Flux Chambers, Anchored Funnels, and Boundary Model Calculations: A
530 Comparison, *Environ. Sci. Technol.*, 46, 4515-4522, <https://doi.org/10.1021/es203465x>, 2012.
- 531 Søndergaard, M., Jeppesen, E., Peder Jensen, J., and Lildal Amsinck, S.: Water Framework Directive:
532 ecological classification of Danish lakes, *J. Appl. Ecol.*, 42, 616-629, <https://doi.org/10.1111/j.1365-2664.2005.01040.x>, 2005.
- 534 Søndergaard, M., Nielsen, A., Skov, C., Baktoft, H., Reitzel, K., Kragh, T., and Davidson, T. A.: Temporarily
535 and frequently occurring summer stratification and its effects on nutrient dynamics, greenhouse gas
536 emission and fish habitat use: case study from Lake Ormstrup (Denmark), *Hydrobiologia*, 850, 65-79,
537 <https://doi.org/10.1007/s10750-022-05039-9>, 2023.
- 538 Wanninkhof, R.: Relationship between wind-speed and gas-exchange over the ocean, *J. Geophys. Res.*
539 *Oceans*, 97, 7373-7382, <https://doi.org/10.1029/92jc00188>, 1992.
- 540 Weiss, R. F.: Carbon dioxide in water and seawater: the solubility of a non-ideal gas, *Mar. Chem.*, 2, 203-
541 215, [https://doi.org/10.1016/0304-4203\(74\)90015-2](https://doi.org/10.1016/0304-4203(74)90015-2), 1974.
- 542 Weiss, R. F. and Price, B. A.: Nitrous oxide solubility in water and seawater, *Mar. Chem.*, 8, 347-359,
543 [https://doi.org/10.1016/0304-4203\(80\)90024-9](https://doi.org/10.1016/0304-4203(80)90024-9), 1980.
- 544 West, W. E., Coloso, J. J., and Jones, S. E.: Effects of algal and terrestrial carbon on methane production
545 rates and methanogen community structure in a temperate lake sediment, *Freshw. Biol.*, 57, 949-955,
546 <https://doi.org/10.1111/j.1365-2427.2012.02755.x>, 2012.



- 547 Wiesenburg, D. A. and Guinasso, N. L.: Equilibrium solubilities of methane, carbon monoxide, and
548 hydrogen in water and sea water, *J. Chem. Eng. Data* . 24, 356-360,
549 <https://doi.org/10.1021/je60083a006>, 1979.
- 550 Wik, M., Crill, P. M., Varner, R. K., and Bastviken, D.: Multiyear measurements of ebullitive methane flux
551 from three subarctic lakes, *J. Geophys. Res. Biogeosci.* . 118, 1307–1321,
552 <https://doi.org/10.1002/jgrg.20103>, 2013.
- 553 Woolway, R. I. and Merchant, C. J.: Worldwide alteration of lake mixing regimes in response to climate
554 change, *Nat. Geosci.*, 12, 271-276, <https://doi.org/10.1038/s41561-019-0322-x>, 2019.
- 555 Yvon-Durocher, G., Allen, A. P., Montoya, J. M., Trimmer, M., and Woodward, G.: The temperature
556 dependence of the carbon cycle in aquatic ecosystems, *Adv. Ecol. Res.*, 43, 267-313,
557 <https://doi.org/10.1016/B978-0-12-385005-8.00007-1>, 2010.
- 558 Yvon-Durocher, G., Allen, A. P., Bastviken, D., Conrad, R., Gudas, C., St-Pierre, A., Thanh-Duc, N., and del
559 Giorgio, P. A.: Methane fluxes show consistent temperature dependence across microbial to ecosystem
560 scales, *Nature*, 507, 488-491, <https://doi.org/10.1038/nature13164>, 2014.
- 561 Zhou, Y., Zhou, L., Zhang, Y., de Souza, J. G., Podgorski, D. C., Spencer, R. G. M., Jeppesen, E., and
562 Davidson, T. A.: Autochthonous dissolved organic matter potentially fuels methane ebullition from
563 experimental lakes, *Water Res.*, 166, 115048, <https://doi.org/10.1016/j.watres.2019.115048>, 2019.
- 564
- 565
- 566



567 Table 1. Summary lake information, summer mean values of a range of variables

Variable	Year
	2020
Secchi depth (m)	0.88
Chlorophyll a ($\mu\text{g/l}$)	52
pH	7.7
Total phosphorus (mg/l)	0.58
Total nitrogen (mg/l)	1.50
TN:TP (by weight)	2.6

568

569 Table 2. Mean greenhouse gas flux (units CO_2 : $\text{mg CH}_4\text{-C m}^{-2} \text{ day}^{-1}$, N_2O : $\text{mg N}_2\text{O -N m}^{-2} \text{ day}^{-1}$ CH_4 both
 570 diffusive and ebullitive in $\text{mg CH}_4\text{-C m}^{-2} \text{ day}^{-1}$) from the lake from spring to Autumn 2020. The emissions
 571 are divided in diffusive, ebullitive emissions. The mean values for all the surface water stations and all
 572 four transects of chambers are given. Mixed stratified versus phases and there SD are also given.
 573 Ebullition is collected for a period covering two weeks so on a number of occasion covered both mixed
 574 and stratified periods and so for ebullition a third category where both mixed and stratified conditions
 575 occurred is given.

576

Emission type	gas	mean	mixed	Stratified	Strat and mixed
	CO_2	506.14	616.6	446.1	



Diffusive		(520.24)	(399.5)	(571.7)	
	CH ₄	9.05 (16.1)	5.9 (3.84)	10.7 (20.40)	
	N ₂ O	0.10 (0.097)	0.083 (0.082)	0.12 (0.10)	
Ebullition	CH ₄	16.99 (19.39)	4.84 (3.27)	47.26 (21.67)	12.78 (10.34)

577

578



579 Figure legends

580 Figure 1. Ormstrup lake bathymetry and sampling stations for surface water greenhouse gas sampling
581 (St1, St2, St3) bottom waters were sampled at S3. Transects of 10 bubble traps were placed on T1- T4.
582 Adapted from the Søndergaard et al. 2023.

583 Figure 2 Temperature profile from June 2020 when the buoy was deployed and surface and bottom water
584 oxygen from June to the end of September 2020. Manual chlorophyll-a ($\mu\text{g L}^{-1}$) values are also given in
585 the top panel.

586 Figure 3. Dissolved CH_4 concentrations from surface and bottom waters – thermal stratification periods
587 highlighted in grey and the white background indicate mixed waters

588 Figure 4 . Dissolved CO_2 concentrations from surface and bottom waters–thermal stratification periods
589 highlighted in grey and the white background indicate mixed waters

590 Figure 5 Dissolved N_2O gas concentrations surface and bottom thermal stratification periods highlighted
591 in grey and the white background indicate mixed waters

592 Figure 6. Ormstrup lakesurface fluxes of the CH_4 , CO_2 and N_2O gases based on dissolved concentration ,
593 thermal stratification periods highlighted in grey and the white background indicate mixed waters

594 Figure 7. Plot of CH_4 ebullition averaged for each transect (10 chambers per transect), data collected from
595 40 traps every two weeks. thermal stratification periods highlighted in grey and the white background
596 indicate mixed waters.

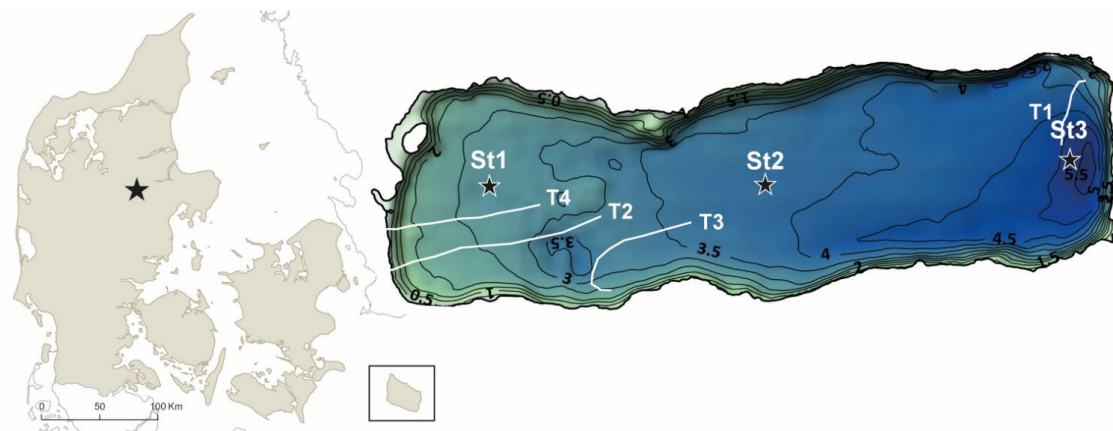
597 Figure 8 – Total lake emissions per gas over the growing season in CO_2 equivalents. The emissions are
598 divided different emission modes: Diffusive, ebullitive and turnover flux.

599 Figure 9. Summary of the quantities of the gases present in the water and the volumes emits from the
600 different pathways. The size of the arrow is proportional to the emissions from each pathway and with the
601 stratified state on the left and the mixed state on the right, with the turnover flux in the centre.



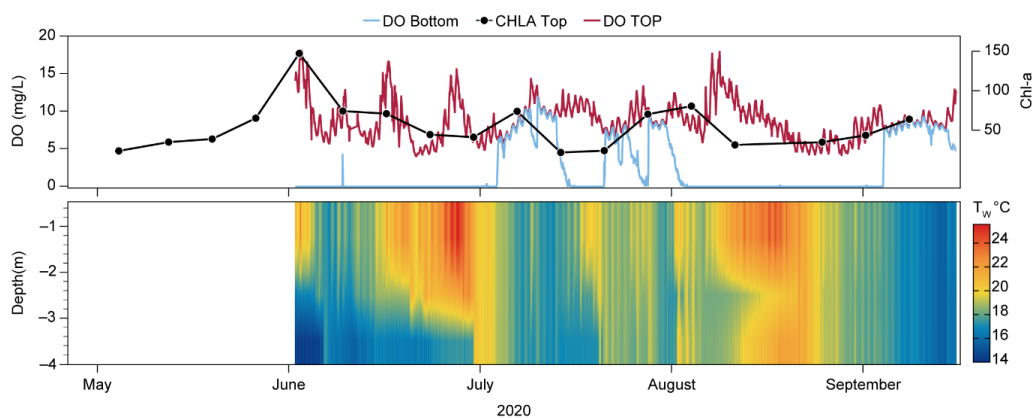
602 Figures and legends

603 Figure 1.



604

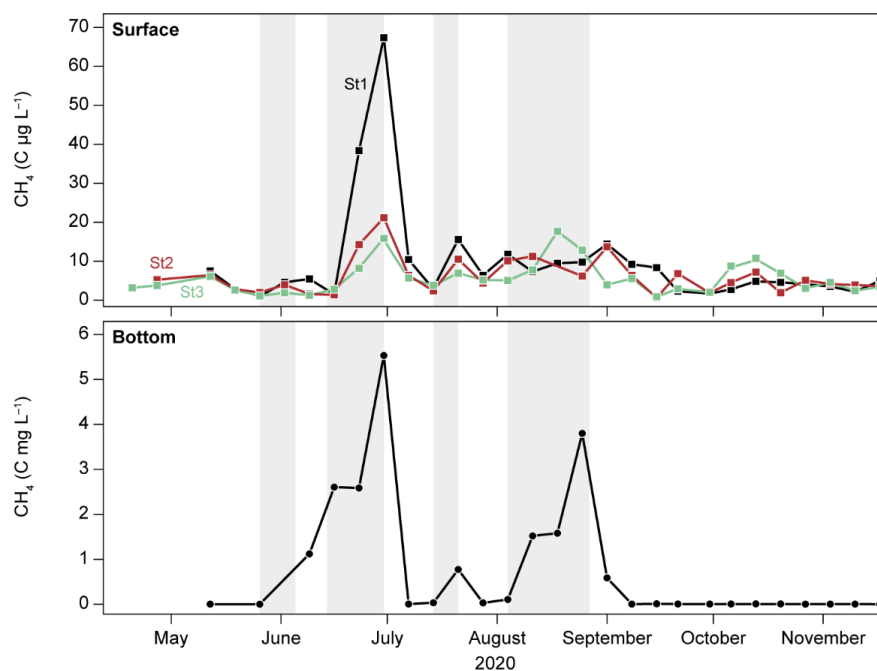
605 Figure 1. Ormstrup lake bathymetry and sampling stations for surface water greenhouse gas sampling (S1,
606 S2, S3) bottom waters were sampled at S3. Transects of 10 bubble traps were placed on T1- T4. Adapted
607 from the Søndergaard et al. 2023.



608

609 Figure 2 Temperature profile from June when the buoy was deployed and surface and bottom water
610 oxygen from June to the end of September. Manual chlorophyll-a ($\mu\text{g L}^{-1}$) values are also given in the top
611 panel.

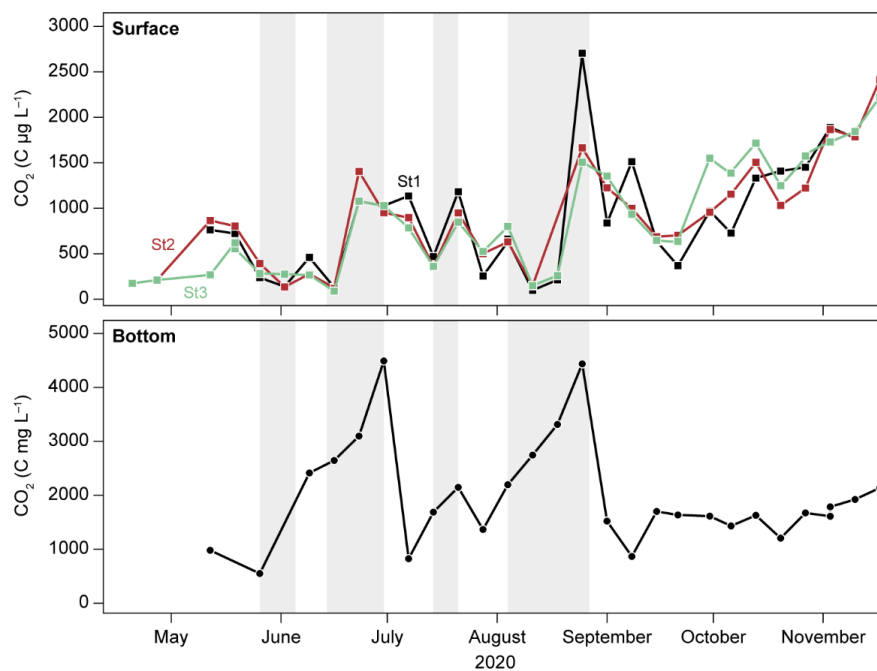
612



613

614 Figure 3. Dissolved CH₄ concentrations from surface and bottom waters – thermal stratification periods

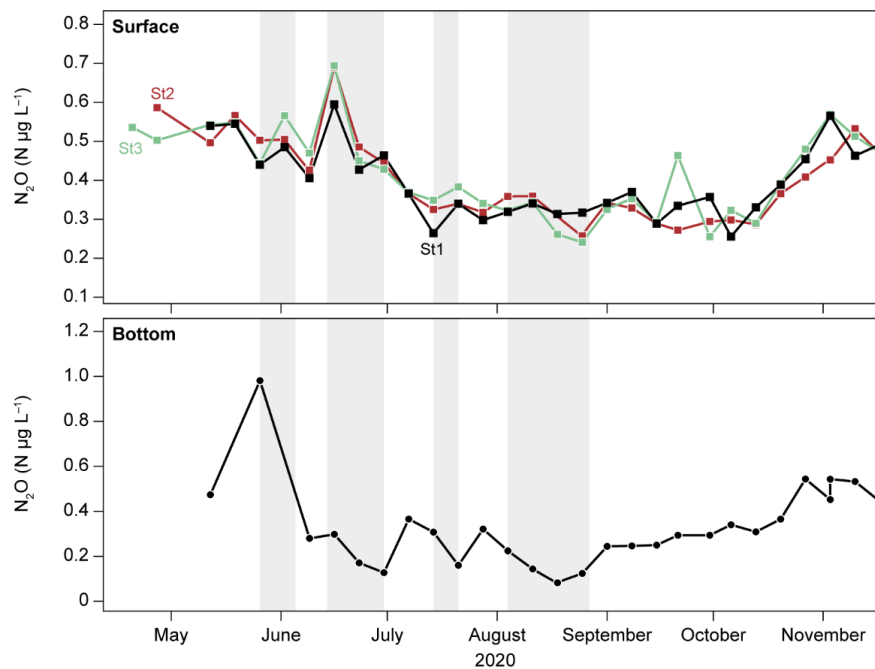
615 highlighted in grey; white background indicate mixed waters



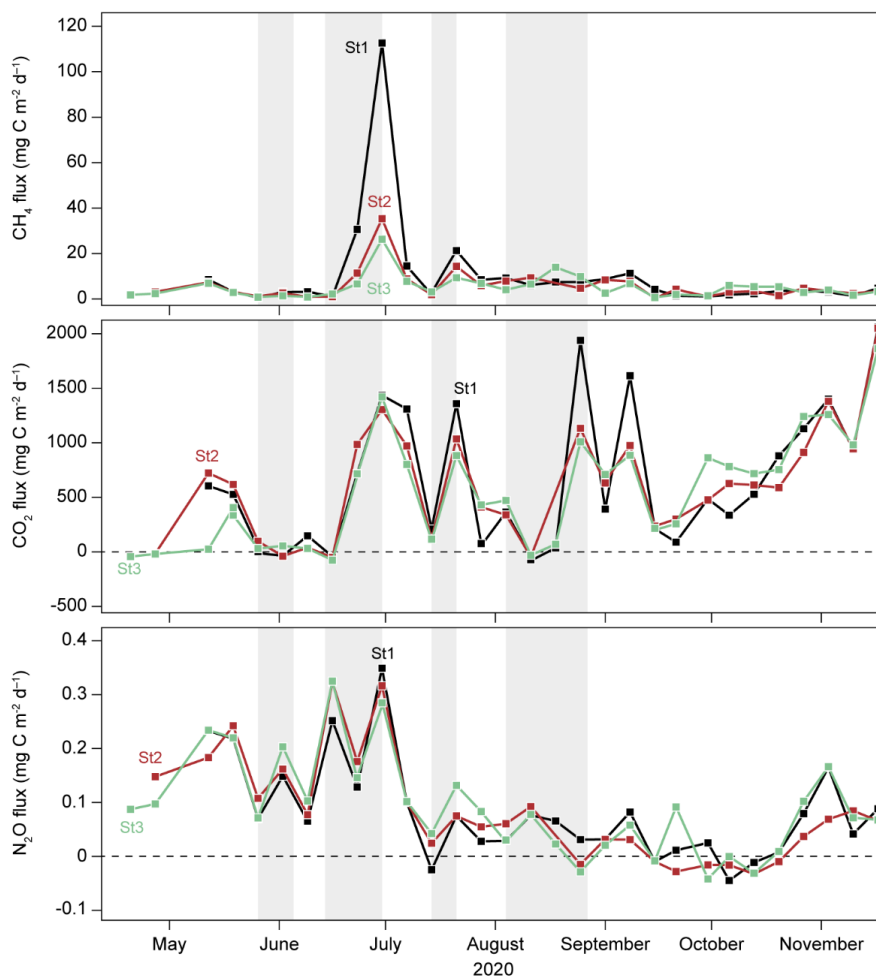
616



617 Figure 4 . Dissolved CO₂ concentrations from surface and bottom waters–
618 thermal stratification periods highlighted in grey; white background indicate mixed waters



619
620 Figure 5 Dissolved N₂O gas concentrations surface and bottom thermal stratification periods highlighted
621 in grey; white background indicate mixed waters



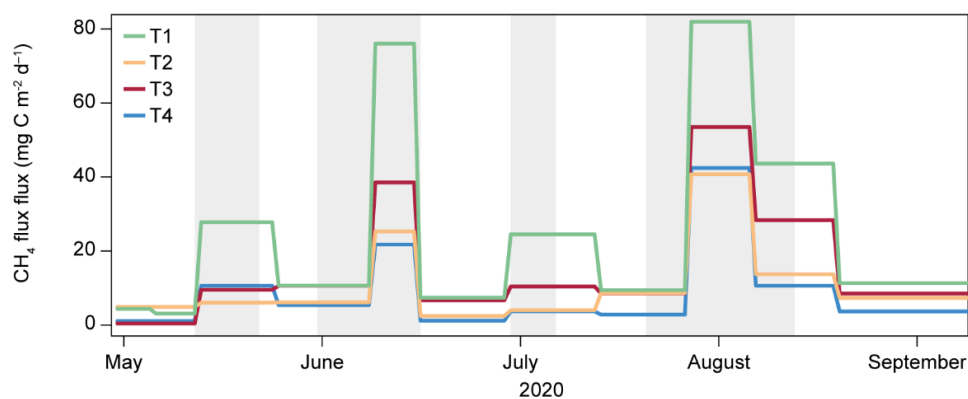
622

623 Figure 6. Omstrup lakesurface fluxes of the CH₄, CO₂ and N₂O gases based on dissolved concentration,
624 thermal stratification periods highlighted in grey; white background indicate mixed waters

625



626



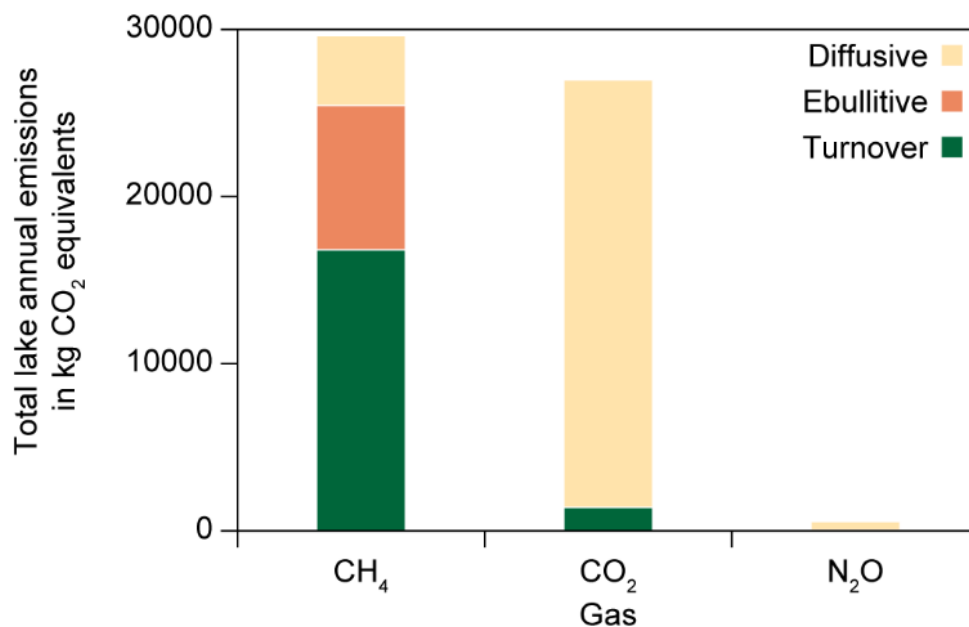
627

628 Figure 7. Plot of CH₄ ebullition averaged for each transect (10 chambers per transect), data collected from
629 40 traps every two weeks. thermal stratification periods highlighted in grey; white background indicate
630 mixed waters.

631

632

633



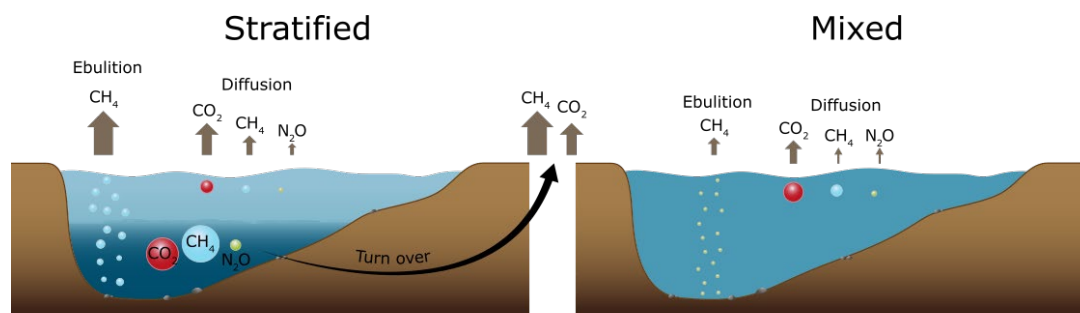
634

635 Figure 8 – Total lake emissions per gas over the growing season in CO₂ equivalents. The emissions are
636 divided different emission pathways: Diffusive, ebullitive and turnover flux.



637

638



639

640 Figure 9 Summary of different flux types (bubble, diffusive and turnover) for the main greenhouse gases

641 (CH₄ CO₂ and N₂O) observed between the stratified and mixed phases at Ormstrup lake patterns in the

642 stratified and mixed phase. The turnover flux of CH₄ and CO₂ is also represented. The size of the arrow

643 represents the relative amount of emission and the size of the circle in the lake represents the

644 concentration of dissolved gases in stratified or mixed water column.

645